Additively Manufactured Flexible Material Characterization and On-demand “Smart” Packaging Topologies for 5G/mmwave Wearable Applications

Kexin Hu[1] Yi Zhou[2] Suresh K. Sitaraman[2] Manos M. Tentzeris[1]

[1]*School of Electrical and Computer Eng.*
Georgia Institute of Technology
Atlanta, USA
khu63@gatech.edu

[2]*George W. Woodruff School of Mechanical Eng.*
Georgia Institute of Technology
Atlanta, USA

2023 IEEE 73rd Electronic Components and Technology Conference (ECTC) | 979-8-3503-3498-2/23/$31.00 ©2023 IEEE | DOI: 10.1109/ECTC51909.2023.00079

***Abstract*—Additively manufactured materials are key components in Flexible Hybrid Electronic (FHE) designs. Accurate characterizations of electrical and mechanical properties for these emerging flexible materials are critical for future wearable 5G/mmWave technologies. This paper investigated 6 types of 3D printed flexible materials including both SLA printed and FDM printed materials. The dielectric constant and loss tangent of these materials over 26-40GHz were extracted from measurements of material samples using Transmission/Reflection method through WR28 waveguide. Universal testing machine and 2D digital imaging correlation (DIC) system were also performed to obtain mechanical properties such as elastic modulus, percent elongation at break,nominal tensile strength and Poisson’s ratios. Among all the tested materials, Polypropylene (PP) demonstrates a very low loss tangent of 0.001, with an elastic modulus of 230 MPa, and a Poisson’s ratio of 0.40, making it an excellent candidate for mmWave flexible and wearable SoP modules. In addition, Silver Nano Particle (SNP) ink and Particle Free Silver (PFS) ink were evaluated for their conductivity and inkjet printability on the 3D printed flexible materials. Inkjet printed microstrip line samples were fabricated on PP substrates with different metallization thickness to measure the insertion loss. With 6 layers of SNP ink, the average deembedded insertion loss is less than 0.1dB/mm. Finally, based on the characterized results and previous work, a “smart” packaging topology including phased array antenna and microfluidic channel with flexible encapsulation is proposed, providing a proof-of-concept demonstration of a flexible wireless wearable electronics platform for high speed data transmission utilizing rapid, low-cost additive manufacturing tools.**

***Index Terms*—additive manufacturing, 3D printing, inkjet printing, 5G/mmWave**

I. Introduction

With the recent development of broadband 5G/mmWave technologies, there is a promise of ultra-high data rates and next-generation data-driven Internet of Things (IoT) systems. In particular, wearable 5G/mmWave technologies are highly desirable for various applications such as ubiquitous health monitoring or activity tracking [1]. The main requirements for future 5G/mm-wave System-on-Package (SoP) design include beam steering antenna arrays operating within broad bandwidth for MIMO systems, reliable interconnects with low parasitic losses at mm-Wave frequencies, and multilayer Multi-chip Module (MCM) integration with high volumetric utilization so that more functionalities can be packed within compact modules [2]. Additionally, these wearable systems should have conformal form-factors with performance that is resilient and adaptable to bending and on-body effects from both RF and mechanical perspectives [3]. Addressing these challenges, this paper discusses fundamental additively manufactured (inkjet/3D printed) flexible materials and next-generation SoP design with on-demand “smart packaging” structures to create flexible, wearable, and integrated wireless electronics.

For 3D printed materials to be used for wearable RF/mmwave applications, it is significant to accurately characterize their dielectric properties including dielectric constant and loss tangent, as well as mechanical/flexing performance for different radii of curvature for frequencies up to above 40GHz. In this work, common 3D printed materials from different companies were chosen in order to characterize both electrical and mechanical properties of interest. Transmission/Reflection method was conducted using WR28 waveguide and dielectric properties were extracted using Nicolson-Ross-Weir (NRW) method. Uniaxial stretching by universal testing machine was also performed to obtain mechanical properties, including elastic modulus, percent elongation at break, and nominal tensile strength. By engaging a 2D digital imaging correlation (DIC) system, the Poisson’s ratios of different dielectrics were also obtained from the uniaxial stretching test. In order to utilize 3D printed low loss materials as substrates for flexible electronics, the fabrication process of inkjet printing conductive ink onto flexible 3D printed substrates was also characterized. In this effort, two types of conductive ink: Silver Nano Particle (SNP) ink (EMD5730) from Suntronic Chemical and a Particle-Free Silver ink (PFS) from Electroninks were considered to compare the conductivity, adhesion and printability. Typically, the surface roughness of substrates varies with different 3D printed materials and significantly affects the printability of the ink, an effect that was success-

2377-5726/23/$31.00 ©2023 IEEE
DOI 10.1109/ECTC51909.2023.00079

Authorized licensed use limited to: Georgia Institute of Technology. Downloaded on November 03,2023 at 01:26:47 UTC from IEEE Xplore. Restrictions apply.

fully alleviated by sanding the surface, printing SU8 layers before the ink deposition and applying UVO treatment. To further investigate the performance of inkjet printed circuits on flexible 3D printed substrates, microstrip lines of variable conductor thicknesses were designed and printed with SNP ink and measured by Vector Network Analyzer. Proof-of-concept prototypes showed that inkjet printed microstrip line on 3D printed Polypropylene substrate can reach less than 0.1dB/mm insertion loss for 24-40GHz frequency band up to 1 inch radius of curvature. Based on the characterized fabrication process, this paper also introduces fully printed wearable multilayer "smart" packaging structures and SoP modules that can integrate antenna on-package, sensors and microfluidic channel connected to microcontrollers with printed rugged interconnects.

II. Electrical properties of 3D printed flexible Materials

Dielectric properties of substrate materials are critical for flexible hybrid electronic designs. There are various methods to measure the properties of dielectric materials. The choice of measurement techniques depends on the kind of material and its application [4]. Transmission/reflection method was used in this paper for wideband characterization covering 26-40GHz, utilizing WR28 waveguides (3.556mm*7.112mm) to measure transmission coefficient(S21) and reflection coefficients(S11) over different materials. This was achieved by measuring samples of 3D printed materials through a Shockline 552B Vector Network Analyzer. The 2 ports of the VNA were first calibrated using A-INFOMW Waveguide Calibration Kits, with short, short, load and thru standards. The waveguide sample holder of 2.99mm thickness was used to hold the printed material samples, therefore, all the materials under test were 3D printed as small cubes in the size of 3.556mm*7.112mm*2.99mm to fit in the sample holder. 6 different 3D printed flexible materials were considered: Flexible 80A and Elastic 50A from Formlabs 3 (SLA printer); TPU 95A, Polypropylene, Soft PLA and Ninjaflex TPU from Ultimaker S3 (FDM printer). The waveguide with sample holder and the system setup are shown in Fig. 1 (a). Fig. 1 (b) shows 3D printed samples of various materials for measurements.

Combining the measured S parameter results of material samples and the results of an empty sample holder, the dielectric constant and loss tangent for each material were derived from a Matlab program. The program utilized the Nicolson-Ross-Weir (NRW) method, which is a standard technique for calculating the dielectric properties of homogeneous, isotropic materials from S11 and S21 [5]. At least three samples were measured for each material and the derived properties were considered in average values. The extracted properties over 26-40GHz frequency band are presented in Fig. 2, and the average values are summarized in Table I. For all the materials, the standard deviations of the dielectric properties between different samples are below 0.1. The dielectric properties of these materials show very few variations in the 26-40GHz

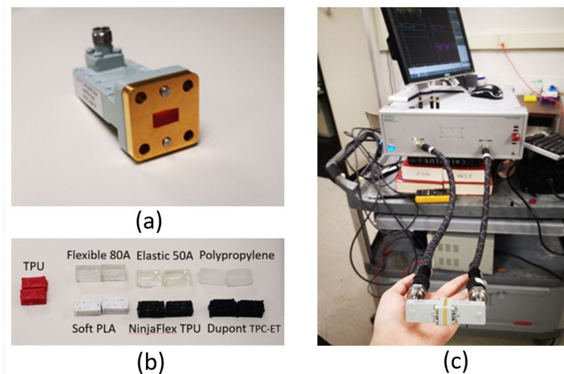

Fig. 1: Waveguide measurements for material characterization. (a) WR28 waveguide with sample holder. (b) 3D printed material samples. (c) Measurement setup

frequency band. Flexible 80A and Elastic 50A materials have larger dielectric constant. Polypropylene (PP) material from Ultimaker features a very low loss tangent of 0.001, which is preferred for mmW flexible modules.

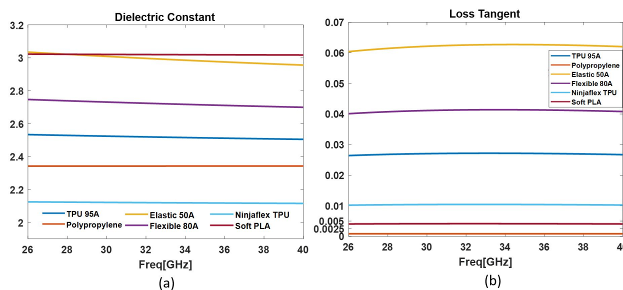

Fig. 2: Dielectric properties of 3D printed flexible materials over 26-40GHz. (a) Dielectric Constant. (b) Loss Tangent.

TABLE I: Dielectric properties of 3D printed flexible materials

Material	Dielectric Constant	Loss Tangent	Surface Roughness Rq(μm)
Flexible 80A	2.73	0.041	0.641
Elastic 50A	3	0.062	0.902
TPU 95A	2.52	0.027	5.68
Polypropylene	2.34	0.001	0.063
Soft PLA	3.02	0.004	0.312
Ninjaflex TPU	2.12	0.01	1.74

Surface roughness is also a key factor when considering 3D printed materials, because it can affect the conductor loss when combining with inkjet printing, especially for mmwave applications [6]. 3D printers like FDM printers usually print with patterns that cause uneven surfaces. To acurately capture the surface morphology and evaluate the properties of different materials, a profilometer was used to measure the surface roughness. The calculated roughenss Rq is recorded in Table I. SLA printed materials tend to have smoother surface compared

Authorized licensed use limited to: Georgia Institute of Technology. Downloaded on November 03,2023 at 01:26:47 UTC from IEEE Xplore. Restrictions apply.

to FDM printed materials. PP shows the lowest roughness among all the materials.

III. Mechanical properties of 3D printed flexible Materials

The mechanical properties of 3D printed flexible materials are significant to design flexible electronics. Since the 3D printed materials are serving as substrates, their mechanical properties will limit the applications of the flexible electronic systems. A uniaxial stretching test was performed by universal testing machine to get the stress-strain curve, from which elastic modulus, percent elongation at break, and tensile strength (nominal) can be obtained. The experimental setup is shown in Fig. 3-a. By engaging a 2D digital imaging correlation (DIC) system, the Poisson's ratios of different dielectric materials are also obtained from the uniaxial stretching tests, as shown in Fig. 3-b. The loading rate applied in all uniaxial stretching tests is 25 mm/min. All six types of 3D printed materials presented in the last section were characterized. The standard size of samples has a width of 25 mm and an effective length of 100 mm. The standard size was used for 80A, 50A, and Soft PLA materials to obtain the stress-strain curve. Since other materials are very ductile, to obtain the full stress-strain curve, a smaller size of 6-mm width and 20-mm effective length was used. Each material was characterized with three samples, with an additional one for DIC. There was deviation in the actual printed thickness and the designed thickness, and the stress-strain curves were based on actual printed thickness by measurement. Fig. 4 shows the stress-strain curve of all six materials with their elastic modulus. The elastic modulus of each sample are the average value of the tangent lines of the linear portion of the curves, and the standard deviation values of the elastic moduli are denoted in the plots. Fig. 5 shows the DIC results of all six materials, and the Poisson's ratio (ν) is obtained by ν=-ϵ_{xx} /ϵ_{yy}, where ϵ_{xx} is the average transverse strain across the selected area, and ϵ_{yy} is the average longitudinal strain.

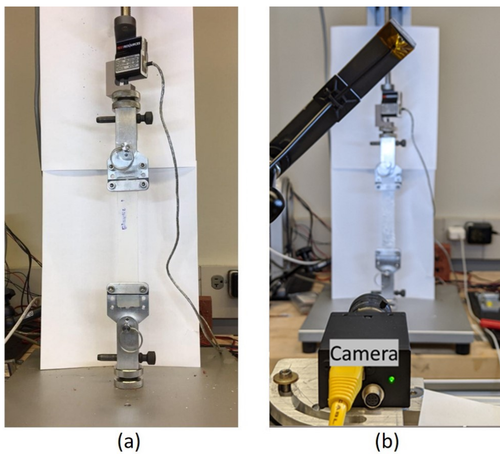

Fig. 3: (a)Uniaxial test setup by universal testing machine with (b) DIC setup with a camera.

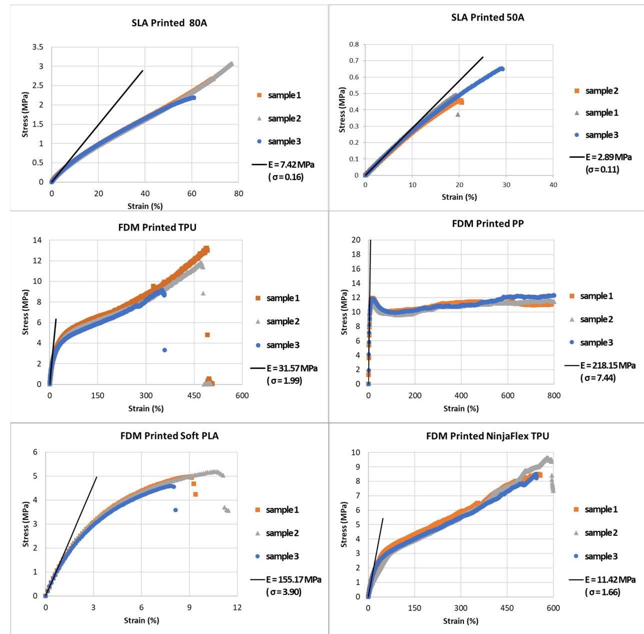

Fig. 4: Stress-strain curve of tested 3D printed materials.

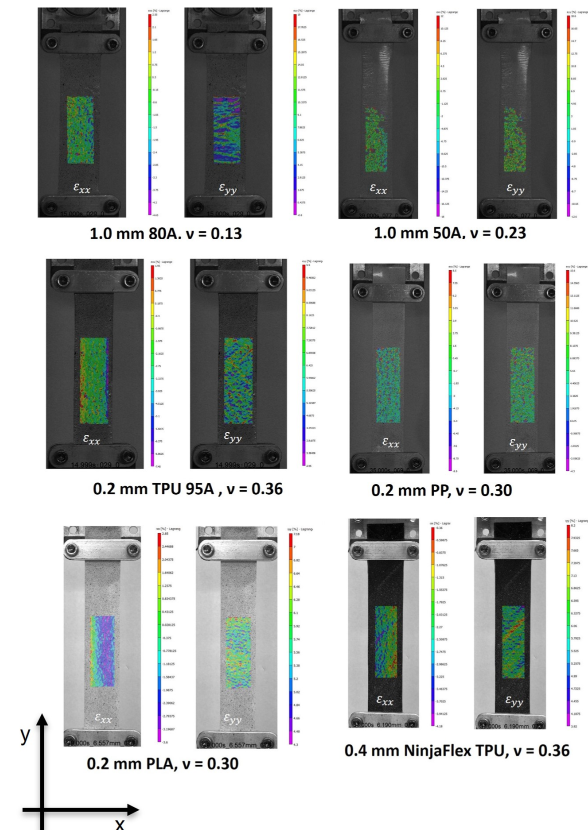

Fig. 5: DIC processed transverse and longitudinal strain distribution of 3D printed materials

The summary of the mechanical properties of all six ma-

Authorized licensed use limited to: Georgia Institute of Technology. Downloaded on November 03,2023 at 01:26:47 UTC from IEEE Xplore. Restrictions apply.

terials is presented in Table II. The Elastic modulus is the average value of three tested samples, and nominal tensile strength and percent elongation at break are taken from the minimal values among three tested samples. The tested Young's moduli and Poisson's ratios are within the reasonable region of their corresponding material types. Many factors could impact the mechanical properties of polymers, including rate of deformation, temperature and chemical nature of the environment [7]. SLA printed materials' mechanical properties are impacted by the layer height, build orientation, washing time, curing time, curing temperature and more [8]. FDM printed materials' mechanical properties are impacted by the printing nozzle temperature, air gap, layer height, infill design, build orientation , raster angle, printing speed and more [9]. All six tested 3D printed materials are commercially available. In this work, SLA printed substrates were set to have layer height of 0.1 mm, and all others are settings were left as the default setting for corresponding material. For FDM printed substrates, they were printed with a zigzag pattern and 100% infill under the default settings for corresponding materials. It is also difficult to compare the same type of materials from different 3D printing manufacturers due to the difference in fabrication process and material composition. Understanding how the mechanical properties would change under different printing setting is not a focus of this work.

TABLE II: Sample Thickness and Mechanical Properties of 3D Printed Materials.

Material	Design Thickness (mm)	Actual Thickness (mm)	Elastic Modulus (MPa)	Poisson's Ratio	Nominal Tensile Strength (MPa)	Nominal Elongation at Break (%)
Flexible 80A	1.0	0.90	7.42	0.13	2.18	60
Elastic 50A	1.0	1.40	52.89	0.23	0.45	20
TPU 95A	0.2	0.27	31.57	0.36	0.80	350
PP	0.2	0.25	218.15	0.30	NA	NA
Soft PLA	0.2	0.24	155.17	0.30	4.56	8
Ninja Flex TPU	0.4	0.28	11.42	0.36	8.23	550

FHE might undergoes different strain values as the application differs. With the tested mechanical properties, one can easily choose a proper substrate based on the strain value it would undergo. And these tested mechanical material properties can be applied to mechanical finite element analysis model for the reliability testing [10]. It is seen that PP has the elastic modulus of 230 MPa, and the Poisson's ratio is 0.40. Although limited by the travel distance of the universal testing machine, unlike the other six materials, PP has never reached a breaking stage up to 800% strain. In addition to its good electrical properties, PP shows good capability to cope with extreme deformation, making it a perfect candidate for wearable SoP structures.

IV. Ink characterization

Two types of ink were evaluated for conductivity and elastic modulus, Silver nano particle(SNP) ink EMD5730 from Suntronic and Particle free silver (PFS) ink from Electronink. Fuji Dimatix DMP-2850 inkjet printer and 10pL cartridges were used for inkjet printing. Both inks were printed with 20um drop spacing for 8 layers onto a PET substrate for measurements. SNP ink was sintered under 130 °C for 1 hour and PFS ink was sintered under 160 °C for 30min in the oven. The measured cross sections are shown in Fig. 6.The PFS ink exhibits a strong coffee ring effect where the ink dries unevenly and accumulated primarily along the perimeter of the printed pattern. The measured conductivity is recorded in Table III. The SNP ink has lower conductivity compared to PFS ink. To be an effective conductor at mmWave frequencies, materials need to have not only high conductivity but also thick conductors of at least 3 skin depths [11]. Skin depth is calculated based on operating frequency, conductivity of the conductor and dielectric constant of the substrate. For example, at 30 GHz, SNP ink needs at least 2.205µm, while PFS ink needs to have at least 1.35µm). Considering the coffee ring effect of PFS ink after sintering, it would be difficult to uniformly satify the skin depth requirements in the cross section, and uneven surface would increase conductor loss. Furthermore, the required sintering temperature of the selected PFS ink is much higher than the one required by SNP ink, which could be a challenge to many 3D printed polymer substrates, since they can be very sensitive to thermal treatment. A solution to these challenges is to use UV sintering instead of heat sintering, to avoid any potential thermal damages to the substrate.

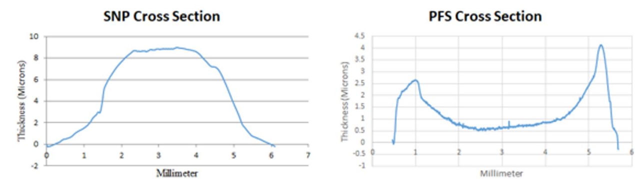

Fig. 6: Cross section measurements of SNP ink and PFS ink

TABLE III: Conductivity and metallization thickness of silver ink

Conductor	Conductivity	Thickness/Layer
SNP ink	$6.68\times10^6 S$	1.1 µm
PFS ink	$1.73\times10^7 S$	varies

The elastic moduli of the two ink were obtained by nanoindentation technique. A 1 cm × 1 cm square was printed using each type of the two inks. The nanoindentation was performed with the Hysitron Triboindenter. By giving a specific force load, the stylus would indent to a corresponding

Authorized licensed use limited to: Georgia Institute of Technology. Downloaded on November 03,2023 at 01:26:47 UTC from IEEE Xplore. Restrictions apply.

depth. Although the material properties are obtained from the unloading portion of the curves, it is critical to make sure that the loading portion of the curves follows the same trend. It is also important to make sure the indentation depth to be much smaller than the thickness of the ink layer. Nine indents are performed to each of the ink with the load linearly increases from 25uN to 100uN. Fig. 7 below shows the valid indentation data, excluding those that do not follow the loading trend, as they might indent into voids of the printed ink. The average elastic modulus value of PFS ink is 2.08 GPa with standard deviation of 0.16 GPa, and the average elastic modulus value of SNP ink is 7.72 GPa with standard deviation of 1.94 GPa.

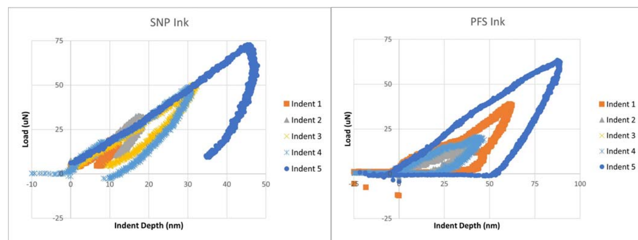

Fig. 7: Nano indentation of the two ink's elastic modulus.

SNP ink was used for further investigation of inkjet printability on different materials. The printing quality of silver ink on 3D printed materials is mainly affected by two factors: surface wetting and surface roughness. Surface wetting can be generally improved by UV Ozone treatment, a simple and effective method for making plastic surfaces more hydrophilic. Different substrates may require different duration of UVO treatment. For PP substrate, it has been proved that 3min of cleaning can achieve the best printing quality for SNP ink [12]. Surface roughness is caused by 3D printing techniques and features, as mentioned in previous sections. An effective way to reduce surface roughness is to sand the surface of these rough materials using a hand sander. For instance, SLA printed materials like Flexible 80A and Elastic 50A adhere very well to SNP ink after sanding. However, for FDM printed materials, sanding is not able to eliminate the uneven pattern caused by printing, therefore, it is necessary to have a buffer layer between silver ink and substrates. SU-8 can be used for this purpose, which is a epoxy-based photoresist that can be cured by a UV crosslinker, with a dielectric constant of approximately 3.2 and a loss tangent of 0.04 at 24.5 GHz [13]. Fig. 8 shows the comparison of surface morphology of inkjet printed silver trace on PP substrate with and without SU8 buffer layers. It is obvious that with SU8 coating, the uneven pattern disappear and the silver trace is much smoother. This will effectively improved the quality of the print, and largely reduce the chance of cracking during bending.

V. "SMART" PACKAGING TOPOLOGIES

Using the fabrication method, microstrip line samples were inkjet printed with SNP ink onto 3D printed PP substrates for characterization of RF performance. As a comparison, microstrip line samples were also fabricated on 3D printed soft

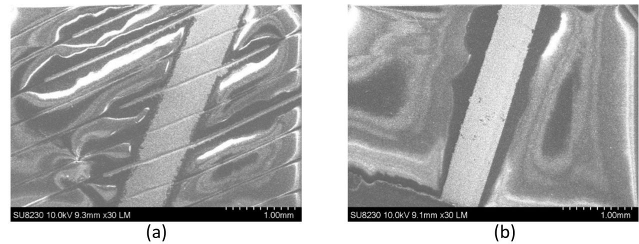

Fig. 8: Comparison of surface morphology of inkjet printed SNP ink on PP substrate. (a) SNP ink trace on PP substrate without SU8. (b) SNP ink trace on PP substrate with SU8.

PLA, PET, RO4350B and RO4003C substrates. The dielectric properties, substrate thickness for each material, as well as the corresponding line width to achieve impedance matching at 50 Ohm are recorded in Table IV. All the samples are 3cm long and measured using the same VNA. The influence of end launch connectors has been removed from deembedding process. The deembedded insertion loss is shown in Fig. 9 and summerized in Table IV. The average S21 is considered to be the mean between the maximum and minimum insertion loss over 20-40GHz. It can be seen that the S21 measurement results agree with the dielectric properties of different substrates. PP demonstrates very low insertion loss of less than 0.1dB/mm up to 40GHz, which is comparable to those commercial RF substrates like RO4003C and RO4350B. Monotonic and cyclic bending tests were also performed with the microstrip line samples on PP substrates to evaluate the reliability in both electrical and mechanical performance. It has been proved that 6 layers of SNP ink can achieve the balance between electrical and mechanical reliability. Detailed measurement results can be found in [10], along with data for conductivity, conductor thickness and SEM examination.

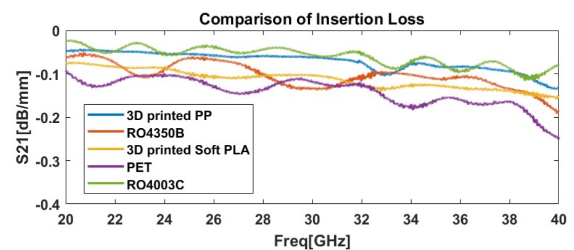

Fig. 9: Comparison of Insertion Loss of inkjet printed microstrip line samples on different substrates

Based on material characterizations and reliability evaluation on interconnects, a "smart" packaging topology and fabrication process are proposed as shown in Fig. 10 and Fig. 11. This platform is a fully wearable integrated front-end, including RF and logic ICs, phased array antenna, packaging and encapsulation, allowing for high data throughput transmit and receive capability. The module is built on 3D printed flexible substrates with embedded microfluidic channels used for thermal management. Necessary surface treatment such as

Authorized licensed use limited to: Georgia Institute of Technology. Downloaded on November 03,2023 at 01:26:47 UTC from IEEE Xplore. Restrictions apply.

TABLE IV: Inkjet Printed Microstrip line Samples on Different Substrates

Material	Dielectric Constant	Loss Tangent	Substrate Thickness	Trace Width	S21 (dB/mm)
Polypropylene	2.34	0.001	0.2	0.55	0.07
Soft PLA	3.01	0.004	0.2	0.5	0.1
RO4350B	3.66	0.0037	0.17	0.35	0.1
RO4003C	3.38	0.0027	0.203	0.47	0.075
PET	2.9	0.008	0.12	0.33	0.15

sanding and UVO cleaning are applied before inkjet printing. Dielectric ink like SU8 material can be used as butter layers for conductive ink to improve printing quality. Multi-chip module integration can be achieved by attaching ICs using conductive epoxy, and inkjet printed interconnects are used for building electrical connections between ICs and external circuits on the substrate. This proposed next generation flexible SoP structure utilizing additive manufacturing, will integrate broadband operation, beamforming capability, low loss rugged interconnects and thermal management in a compact and reliable module.

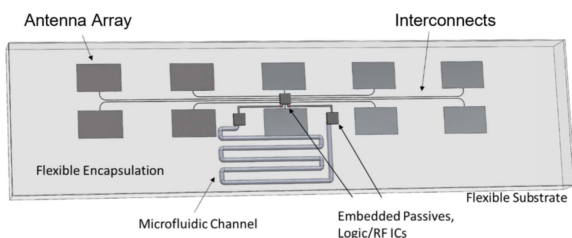

Fig. 10: Proof-of-concept demonstration of "smart" packaging and wearable SoP modules utilizing additive manufacturing

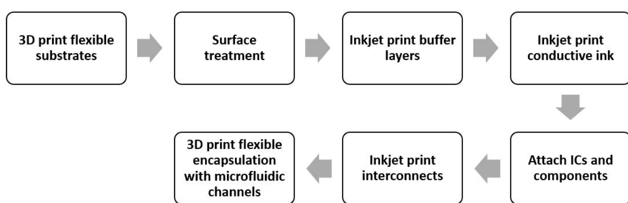

Fig. 11: Fabrication process for inkjet printing onto 3D printed flexible substrates

VI. Conclusions

This paper presents the material characterizations of different types of additively manufactured materials over 24-40GHz covering the 5G/mmWave frequency band. Both electrical properties and mechanical properties were evaluated for 3D printed flexible materials and inkjet printed conductive silver ink. The results showed that Polypropylene (PP) material from Ultimaker, among all other 3D printed materials is a good candidate for mmWave flexible modules, with a low loss tangent of 0.001, an elastic modulus of 230 MPa, and a Poisson's ratio of 0.40. The fabrication process has also been characterized, and the fabricated prototypes of microstrip lines on PP substrates features less than 0.1dB/mm insertion loss up to 40GHz. Previous work also showed that additively manufactured interconnects can maintain a very good performance while withstanding cyclic bending of 1 inch radius over 10000 times [10]. In addition, this work introduces the general fabrication process of inkjet printing onto 3D printed flexible substrate, which is significant to the large-scale implementation of 5G/mmWave flexible MCM modules with low loss and reliable interconnection between chips and circuits. Finally, the results and demonstration from this work would enhance the foundation to improve the efficiency and functionality of flexible additively manufactured RF modules for 5G/mmW MCM and SOP designs.

Acknowledgment

This material is based on research sponsored by Army Research Laboratory under agreement number W911NF-19-2-0345. The U.S. Government is authorized to reproduce and distribute reprints for Government purposes notwithstanding any copyright notation thereon. The views and conclusions contained herein are those of the authors and should not be interpreted as necessarily representing the official policies or endorsements, either expressed or implied, of Army Research Laboratory (ARL) or the U.S. Government.

References

[1] M. Wagih et al., "Microwave-Enabled Wearables: Underpinning Technologies, Integration Platforms, and Next-Generation Roadmap," in IEEE Journal of Microwaves, vol. 3, no. 1, pp. 193-226, Jan. 2023, doi: 10.1109/JMW.2022.3223254.

[2] T. -H. Lin, S. N. Daskalakis, A. Georgiadis and M. M. Tentzeris, "Achieving Fully Autonomous System-on-Package Designs: An Embedded-on-Package 5G Energy Harvester within 3D Printed Multilayer Flexible Packaging Structures," 2019 IEEE MTT-S International Microwave Symposium (IMS), Boston, MA, USA, 2019, pp. 1375-1378, doi: 10.1109/MWSYM.2019.8700931.

[3] N. F. M. Aun, P. J. Soh, A. A. Al-Hadi, M. F. Jamlos, G. A. E. Vandenbosch and D. Schreurs, "Revolutionizing Wearables for 5G: 5G Technologies: Recent Developments and Future Perspectives for Wearable Devices and Antennas," in IEEE Microwave Magazine, vol. 18, no. 3, pp. 108-124, May 2017, doi: 10.1109/MMM.2017.2664019.

[4] Costa F, Borgese M, Degiorgi M, Monorchio A. Electromagnetic Characterisation of Materials by Using Transmission/Reflection (T/R) Devices. Electronics. 2017; 6(4):95. https://doi.org/10.3390/electronics6040095

[5] A. N. Vicente, G. M. Dip and C. Junqueira, "The step by step development of NRW method," 2011 SBMO/IEEE MTT-S International Microwave and Optoelectronics Conference (IMOC 2011), Natal, Brazil, 2011, pp. 738-742, doi: 10.1109/IMOC.2011.6169318.

[6] Ying Ying Lim, Yee Mey Goh, and Changqing Liu, Industrial & Engineering Chemistry Research, 2013-52 (33), 11564-11574, DOI: 10.1021/ie4006639.

[7] B. Vo, A. Ajibade, M. Rosengren, K. Pena, and M. Moran, "The effect of 3D printing temperature on the mechanical properties of polypropylene." Journal of Undergraduate Chemical Engineering Research 8, no. 1 (2019): 24-31.

[8] A. Pandzic, "Influence of layer height, build orientation and post curing on tensile mechanical properties of SLA 3D Printed material," Proceedings of the 32nd International DAAAM Symposium 2021, pp. 0200–0208, 2021.

Authorized licensed use limited to: Georgia Institute of Technology. Downloaded on November 03,2023 at 01:26:47 UTC from IEEE Xplore. Restrictions apply.

[9] A. Pandzic and D. Hodzic, “Mechanical properties comparison of PLA, Tough Pla and PC 3D printed materials with infill structure – influence of infill pattern on tensile mechanical properties,” IOP Conference Series: Materials Science and Engineering, vol. 1208, no. 1, p. 012019, 2021.
[10] Y. Zhou, K. Hu, M. M. Tentzeris and S. K. Sitaraman, ”Mechanical and Ka-Band Electrical Reliability Testing of Interconnects in 5G Wearable System-on-Package Designs Under Bending,” 2022 IEEE 72nd Electronic Components and Technology Conference (ECTC), San Diego, CA, USA, 2022, pp. 914-923, doi: 10.1109/ECTC51906.2022.00149.
[11] V. V. M. Elwyn, “Fundamentals of Networks,” in Reference data for Engineers: Radio, electronics, computer, and Communications, Boston: Newnes, 2002, pp. 6–1-6–22.
[12] K. Hu, Y. Zhou, S. K. Sitaraman and M. M. Tentzeris, ”Fully Additively Manufactured Flexible Dual-Band Slotted Patch Antenna for 5G/mmwave Wearable Applications,” 2022 IEEE International Symposium on Antennas and Propagation and USNC-URSI Radio Science Meeting (AP-S/URSI), Denver, CO, USA, 2022, pp. 878-879, doi: 10.1109/AP-S/USNC-URSI47032.2022.9886082.
[13] B. K. Tehrani and M. M. Tentzeris, ”Fully Inkjet-Printed Ramp Interconnects for Wireless Ka-Band MMIC Devices and Multi-Chip Module Packaging,” 2018 48th European Microwave Conference (EuMC), Madrid, Spain, 2018, pp. 1037-1040, doi: 10.23919/EuMC.2018.8541741.

Authorized licensed use limited to: Georgia Institute of Technology. Downloaded on November 03,2023 at 01:26:47 UTC from IEEE Xplore. Restrictions apply.